High Gain DC-DC Converter Fed Six-Step Inverter Based BLDC Motor

Konda Naresh(✉), D. Suresh, and S. Pattnaik

Department of Electrical Engineering, N.I.T, Raipur, Chhattisgarh 492010, India
{knaresh.phd2022.ee,dsuresh.ee,spattnaik.ele}@nitrr.ac.in

Abstract. This paper discusses switched-inductor (SI)-based active-front-end (AFE) converters with a six-step inverter proposed for the speed control of a BLDC motor. The proposed converter is a non-isolated, high-gain converter (HGC). Brushless DC (BLDC) motor speed regulation is obtained by regulating the high-gain DC-DC converter's DC link voltage through the PI controller. Current control is realized with the hysteresis controller. The proposed converter was analyzed in this article, and its performance characteristics were compared with those of the conventional converter. The proposed converter works with less current coming in and less stress on the switching voltage. In the Simpower system blockset, MATLAB/Simulink is used to simulate the characteristics of the adopted converter with a BLDC motor.

Keywords: BLDC Motor · VSI (Voltage Source Inverter) · Voltage Con trol · Current Control · Hysteresis Control · Bidirectional Converter

1 Introduction

A bidirectional converter is used to connect a device that stores energy to a system that makes renewable energy. Charging mode occurs when energy use exceeds supply. On the other hand, the discharging mode is turned on when energy demand is higher than supply, and the batteries send power to the load [1]. In charging modes, battery voltage is minimized to match the DC link and increased if necessary. In discharging modes, the voltage is increased if necessary and decreased if the voltage is less than the DC link [2]. It has the same fundamental modes of operation as any other DC-DC converter. An all-purpose DC-DC converter with both voltages stepping up and down is needed to provide power from the battery while operating in regenerative mode and storing the battery. The bidirectional converter must be able to transform DC bus voltage is converted up into the different battery voltage levels, including both states [3]. Bidirectional DC-DC converters are used in many fields, such as aerospace, UPS, EVs, PV, and other products and services. They can be isolated or non-isolated to serve different purposes [4]. SRM motors, synchronous-RM motors, PMSM motors, IM motors, DC motors, BLDC motors, and axial flux ironless permanent magnet motors are all types of e-motors that can be used in EVs [5]. BLDC is the most ideal for EV applications due to its dispersed BLDC motor windings and trapezoidal current wave pattern without

B. Raj et al. (Eds.): ICETE 2023, AER 223, pp. 662–672, 2023.
https://doi.org/10.2991/978-94-6463-252-1_67

the need for a brush or commutator [6] synchronization. BLDC motors use Hall sensor data on the rotor position to inject a phase sequence synchronized with the back-EMF waveform, used in many industries [7].

With a regenerative braking system, gasoline-powered cars can recover the energy they lose when they stop. This saves fuel and reduces pollution. In hysteresis, the current control technique uses three different ways to measure speed, current, and voltage. The absolute speed is calculated using the speed detector, which is a Hall sensor, and then compared to the selected reference speed. After figuring out how to respond to real changes in speed, the PI regulator will figure out an error signal. The current signal produced by the rectifier is then contrasted with this signal [8].

The paper proposes a high-gain converter (HGC) fed by BLDC motor speed control. The PI controller controls the voltage of the high-gain converter (HGC), which controls the speed of the BLDC drive. The hysteresis controller, which was proposed in this paper, controls the current. This paper is divided into seven parts. Section 2.2 shows how the existing and proposed high-gain converters (HGC) are put together. Section 3 describes the brushless DC motor drive fed with a six-step inverter, while Section 4 describes the BLDC motor drive fed with a proposed high-gain converter (HGC) through a six-step inverter. The next part of this paper is Section 5, "Simulation Results and Discussions," and the last part is the "Conclusion."

2 DC-DC Converters

2.1 Conventional DC-DC Converter

The conventional converter topology circuit is shown in Fig. 1a. The circuit contains one supply source: a battery, an inductor, two controlled switches, and a DC link capacitor across the load. As controlled switch B is turn off, the direction of inductor L is reversed, resulting in current flowing from the inductor to the diode D_A, to the load, and then back to the inductor. The controlled switch A turns on, allowing current to flow from the load to the DC link capacitor, controlled switch A, inductor L, and supply. When controlled switch A is turn off, the direction of the inductor is swapped, and current passes from the inductor to the battery, diode D_B, and returns to the inductor L. The flow of current can be made into 2 states of modes: one is mode-I operation, in which controlled switch B is in conduction mode, and controlled switch B is in non-conduction mode; in this mode, DC

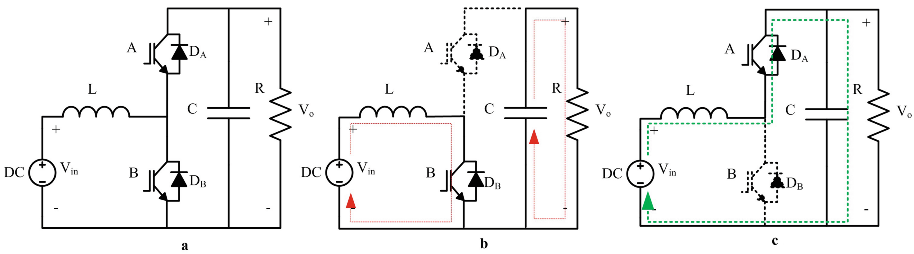

Fig. 1. (a) Conventional Bidirectional DC-DC converter (b) Mode - I Operation, (c) Mode - II Operation

link voltage drives the load; the other is mode-II operation, in which controlled switch A is in conduction mode, and another controlled switch is in non-conducting mode. These two modes of current flow directions are shown in Fig. 1.b, c

Mode- I:

A is in OFF

B is in the ON Mode of operation Where

V_{in} is the input supply voltage

V_L is the Across the voltage

V_C is the Across the Capacitor C voltage

V_o is the Across the Load voltage

Voltage equations of DC-DC converter for Mode -I

$$\begin{aligned} -V_{in} + V_L &= 0 \\ V_L &= V_{in} \\ V_C &= V_{in} \\ L\frac{\mathrm{d}i_L}{dt} &= V_{in} \\ \Delta i_L &= \frac{V_{in}}{L} * Mode_I \end{aligned} \tag{1}$$

Mode- II: A is in ON

B is in the OFF Mode of operation

Voltage equations of DC-DC converter for Mode -II

$$\begin{aligned} -V_{in} + V_L + V_o &= 0 \\ V_L &= V_{in} - V_o \\ L\frac{\mathrm{d}i_L}{\mathrm{d}t} &= V_{in} - V_o \\ \Delta i_L &= \frac{V_{in} - V_o}{L} * Mode_{II} \end{aligned} \tag{2}$$

According to Volt-Sec Balance equation

$$\begin{aligned} &\frac{V_{in}}{L} * DT + \frac{(V_{in} - V_0)}{L} * (1 - D) * T = 0 \\ &V_{in} * D + (V_{in} - V_o) * (1 - D) = 0 \\ &V_{in} = V_o * (1 - D) \\ &\frac{V_o}{V_{in}} = \frac{1}{(1 - D)} \end{aligned} \tag{3}$$

where D is the duty ratio

$$D = 1 - \frac{V_o}{V_{in}}$$

2.2 SI-Based High Gain DC-DC Converter

The system configuration for the proposed converter topology is in Fig. 2a. In this case, a switched inductor is used in place of the inductor to turn the conventional converter into the proposed converter. The supply source, battery, switched inductor structure, two controlled switches, and DC link capacitor are across the load in this circuit. This circuit analysis is in two modes: Mode-I and Mode-II. Here, we understand the working of the switched inductor [9] to be in two modes. They have charging and discharging modes of operation. In the charging mode of operation, the two inductors are in parallel; in this case, D_3 is reverse-biased, so it is in non-conducting mode. Whereas in discharging mode, the two inductors are in series, and the diodes D_1 and D_2 are reverse biased, so these are in the non-conducting mode of operation. In Mode-I, the controlled switch B is in turn-on mode, and another controlled switch is in turn-off mode. In this case, the two inductors are in parallel in a switched inductor structure.

As controlled switch B is turned off, the direction of inductor L is reversed, resulting in current flowing from the inductor to the diode D_A, to the load, and then back to the inductor L (switched inductor). In this mode, the DC link capacitor drives the load. In Mode-II, the controlled switch A is in turn-on mode, and another controlled switch B is in turn-off mode. In this case, in the switched inductor structure, the inductors are in series; in this case, the two inductors discharge through the controlled switch A to the load and return to the supply source. These two modes of current flow directions are shown in Fig. 2b and c.

Mode- I:

A is in OFF

B is in ON Mode of operation

Since the two inductors are in parallel Where

V_{L1} In SI structure Inductor L_1 across voltage V_{L2} In SI structure Inductor L_2 across voltage V_{in} Supply Voltage

V_o Load Voltage

V_L Inductor Across Voltage

V_C Capacitor Across Voltage

Voltage equations of SI-Based DC-DC converter for Mode –I

$$\begin{aligned} V_{L1} &= V_{L2} = V_L \\ -Vin + V_L &= 0 \end{aligned} \tag{4}$$

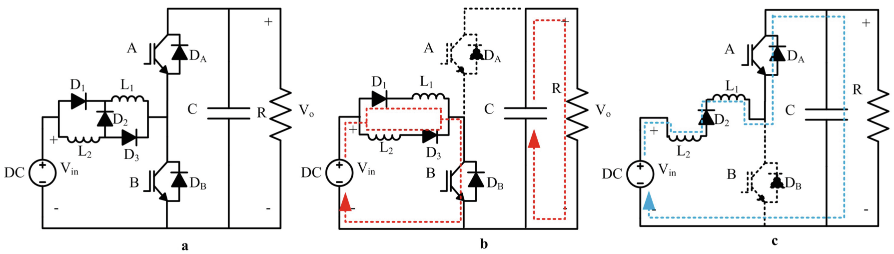

Fig. 2. (a) Proposed HGC, (b) Mode - I Operation, (c) Mode - II Operation

$$V_C = V_o \tag{5}$$

From Equation (4)

$$V_L = V_{in}$$

$$\begin{aligned} L\frac{\mathrm{d}i_L}{\mathrm{d}t} &= V_{in} \\ \Delta i_L &= \frac{V_{in}}{L} * Mode_I \end{aligned} \tag{6}$$

Mode- II:
A is in ON
B is in OFF Mode of operation
Voltage equations of SI-Based DC-DC converter for Mode -II

$$-V_{in} + V_{L1} + V_{L2} + V_o = 0$$

Since the two inductors are in series, so

$$\begin{aligned} V_{L1} + V_{L2} &= 2V_L \\ \Delta i_L &= \frac{(V_{in} - V_o)}{2L} * (1 - D) * T \end{aligned} \tag{7}$$

According to Volt-Sec balance equation

$$\begin{aligned} \frac{V_{in}}{L} * DT + \frac{(V_{in} - V_0)}{2L} * (1 - D) * T \\ \frac{V_o}{V_{in}} = \frac{1 + D}{1 - D} \end{aligned} \tag{8}$$

3 Brushless DC Motor Drive Fed with Six–Step Inverter

BLDC motors are still an excellent alternative to electric cars due to their enhanced power efficiencies, improved speed characteristics, high efficiency, vast speed capabilities, and low servicing. Nevertheless, complicated electronics are required for supervision. BLDC is made up of a rotor and stator, similar to a conventional electrical machine. It is easy to govern (six stages) and utilizes just dc current flow. These are regulated electronic forms, and the current conducting stator conductors are energized in a certain manner. The rotor's orientation must be known in order to choose which winding should be activated next; hence triple hall detectors will be installed in the armature.

Figure 3a depicts the block diagram of a conventional BLDC motor drive; the appropriate output waveform for back-EMF and phase currents are in Fig. 3b, and its six-step commutations are in Table 1. Mathematical modelling Equations of 3-Phase BLDC Motor expressed in Eq. 9, 10 and 11 are

$$V_a = i_a * R_a + L * \frac{\mathrm{d}}{\mathrm{d}t} i_a + e_a \tag{9}$$

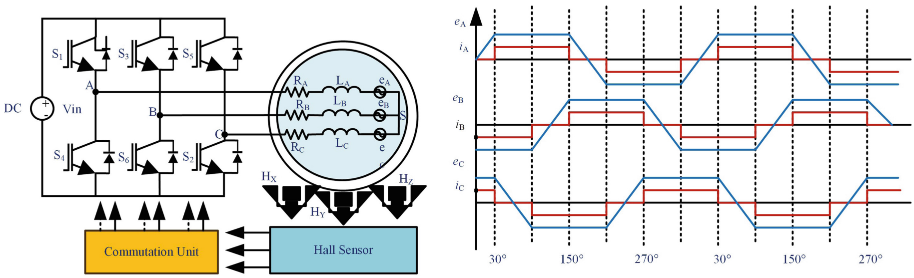

a **b**

Fig. 3. (a) Block diagram of a brushless DC motor, (b) Ideal Back-EMF and Phase Currents of BLDC Motor

Table 1. Six Step Commutation

HX	*HY*	*HZ*	Switching pattern
1	0	1	$S1,S6$
1	0	0	$S1,S2$
1	1	0	$S3,S2$
0	1	0	$S3,S4$
0	1	1	$S5,S4$
0	0	1	$S5,S6$

$$V_b = i_b * R_b + L * \frac{\mathrm{d}}{\mathrm{d}t} i_b + e_b \tag{10}$$

$$V_c = i_c * R_c + L * \frac{\mathrm{d}}{\mathrm{d}t} i_c + e_c \tag{11}$$

where R_a, R_b, R_c Stator resistance of BLDC Motors phase A, B and C
i_a, i_b, i_c Stator Current of BLDC Motors phase A, B and C
L is the Inductance of the Stator winding
e_a, e_b, e_c Stator Back-EMF of BLDC Motors phase A, B and C
The electromagnetic torque equation of the BLDC Motor is given by

$$\tau = \frac{e_a * i_a + e_b * i_b + e_c * i_c}{\omega} \tag{12}$$

where ω is the rotor speed of the BLDC Motor The mechanical torque is

$$T_m = J \frac{\mathrm{d}\omega}{\mathrm{d}t} + B * \omega + T_L \tag{13}$$

where

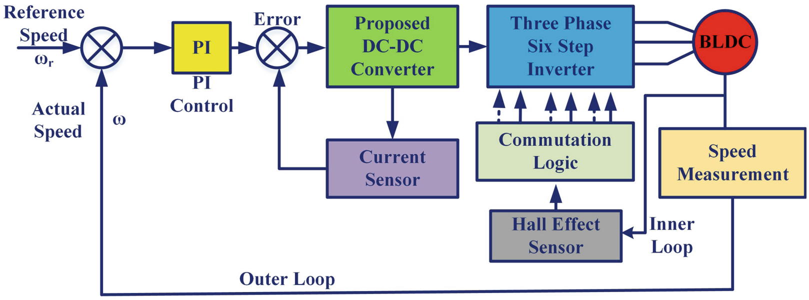

Fig. 4. HGC fed with BLDC motor drive through six-step Inverter

B is the Damping Constant
J is the Rotor Inertia of BLDC Motor
T_L is the Load Torque

4 HGC Fed with BLDC Motor Drive Through Six-Step Inverter

As the rectifier's AC voltage is given straight to VSI, the DC-DC converter with a conventional BLDC control is not required. The supplied voltage is directly proportional to the motor's speed. So, the speed of a conventional BLDC motor is controlled using a PI controller. In this paper, we propose hysteresis control. This control is the most fundamental current control. Two control loops are employed, for the speed of BLDC. The speed control loop is on the outside, while the current control loop is on the inside. The Fig. 4 shows the block diagram of the BLDC motor drive fed with the Proposed DC-DC Converter through the six-step Inverter. Now, the voltage is not directly given to the VSI inverter in the proposed converter. This means that the controlled DC voltage is sent to the VSI inverter in order to control the speed needed for the application. To switch the switches that the gate signals control, the VSI inverter uses the inner closed loop. Another loop is the outer closed loop, which collects the speed of the rotor and compares it with the reference one. It generates the error; it is given to the hysteresis; finally, gate signals are given to the proposed DC-DC converter with a complement to each other. We can observe that from the Table 2, the gain of the proposed converter is increased, so according to the gain, the stress on the controlled switches is reduced. Figure 5 shows the circuit diagram of the HGBC converter fed with a six-step Inverter with an SI structure instead of an inductor in the conventional circuit diagram.

5 Simulation Results and Discussion

The comparison between the two converters is shown in Table 2. We can observe that the proposed converter is more ripple-free and has a high gain. The simulation parameters and their values are shown in Table 3.

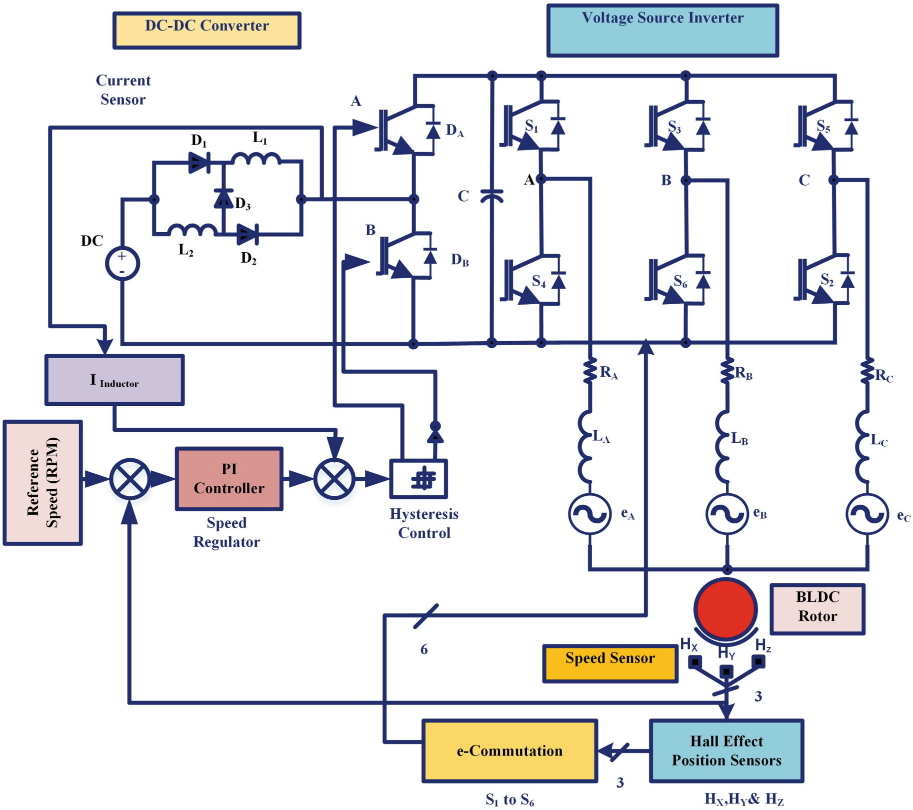

Fig. 5. Block diagram of HGC converter With SI structure

Table 2. Comparison between the two converters

S. No	Name of the Converter	Voltage Gain	DC-DC Converter		BLDC			
			Inductor current (amp)	Converter Voltage (Volts)	Stator Current (amp)	Stator Back-EMF (Volts)	Rotor Speed (rpm)	Torque (Nm)
1	Conventional	1/(1+D)	9.188	406.2	2.2	183.2	2499	3.143
2	HGC	(1+D)/(1−D)	6.094	406.3	0.033	183.3	2500	3.379

5.1 Conventional DC-DC Converter

Figure 5 illustrates the simulated behaviour of a six-step inverter-fed conventional bidirectional converter. In this, BLDC waveforms representing Stator Current (amp), Back-EMF (volt) (that is Phase A), Speed of the BLDC Rotor (rpm), and Torque of the BLDC Motor are input into a conventional DC-DC bidirectional converter. BLDC motor speed control is simulated in MATLAB using Simpower's block set. Using the regulation often

Table 3. Simulation Parameters

DC-DC Converter			BLDC	
S. No.	Name of the Parameter	Value	Name of the Parameter	Value
1	SI L1	20e-3(H)	Stator Phase Resistance Rs	2.6750 (ohm)
2	SI L2	20e-3(H)	Stator Phase Inductance Ls	8.2e-3 (H)
3	Capacitor	2200e-6(F)	Back EMF (Degree)	120

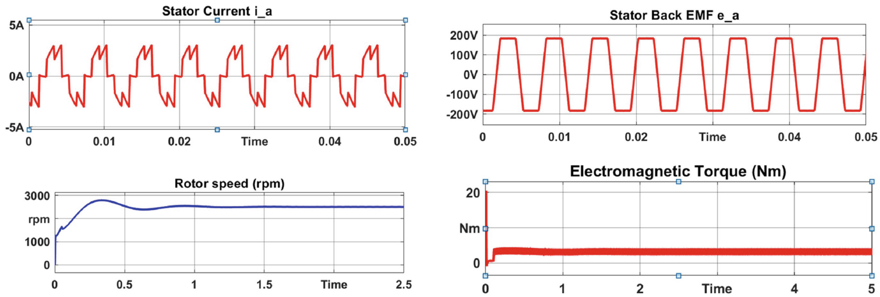

Fig. 6. Conventional DC-DC Converter fed with BLDC waveforms respectively Stator Current, Back-EMF, Rotor Speed and Torque

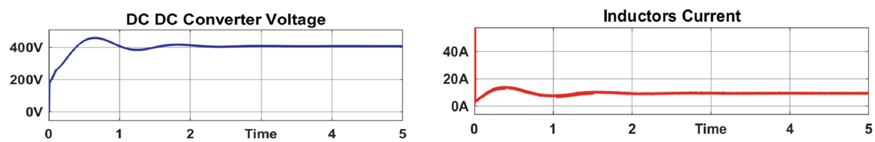

Fig. 7. Conventional Voltage and Inductors Current waveform

utilized blockset of the MAT-LAB Simulink conditions, Outward speed regulator feedback and inward current regulation feedback are created. Power-electronic block sets are used to create the boost converter and inverter. Figure 6, shows the stator current waveform and trapezoidal Back-EMF. The proper commutation order of the hall signals is determined by where the hall sensor is placed. Hall signals are used to create the inverter's switching signal. The voltage of bidirectional converter is used to control BLDC motor's speed. In, Figure 5 shows the indications for speed and torque. Figure 5 shows that the torque created with the bidirectional DC-DC converter-fed BLDC motor includes ripple. Figure 7 shows the conventional DC-DC converter's Voltage and Inductor's Current waveforms. We can observe from Table 2 that the inductor current is and has a high ripple.

5.2 SI-Based HGC Converter

Figure 8 shows the proposed HGBC-fed BLDC motor simulated waveforms, respectively Stator Current i_a, Back-EMF e_a, Rotor Speed (rpm) and Torque (Nm).

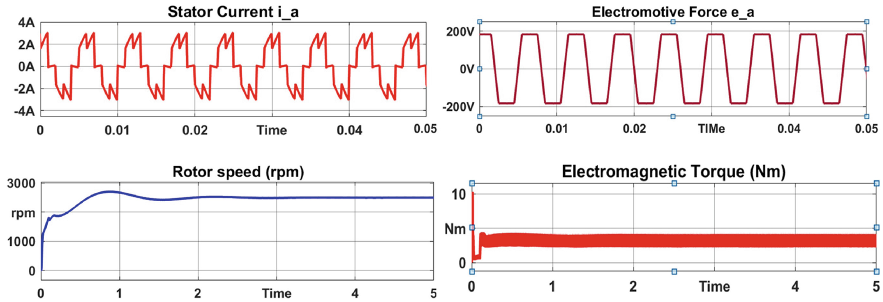

Fig. 8. SI-based HGC fed with BLDC waveforms respectively Stator Current, Back-EMF, Rotor Speed and Torque

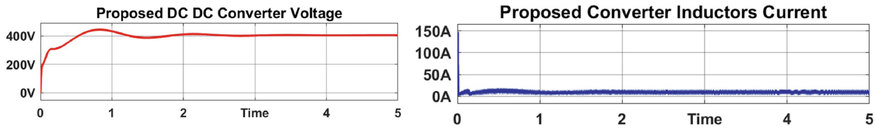

Fig. 9. SI-based HGC Converter Voltage and Inductors Current waveform

High Gain Converter (HGC) converter-fed BLDC with a six-step inverter and Conventional DC-DC converter-fed BLDC motor with a six-step inverter are regulated at the reference speed of 2500 revolutions per minute for BLDC motors. However, the speed and torque of a traditional converter-fed BLDC motor are erratic. The BLDC motor operates noisily when a ripple is present. Toque ripple does not exist in a high gain (HGC) converter-fed BLDC motor. We can be observed that Table 2, is the numerical comparison between the two converters of simulated results. The proposed one has less ripple, and less switched stress on the converters-controlled switch. Figure 9 shows the Proposed DC-DC converter's Voltage and Inductor's Current waveforms. We can observe from Table 2 that the inductor current is and has a high ripple.

6 Conclusion

The switched inductor (SI) based-high gain converter (HGC) with a six-step inverter is used to regulate the BLDC motor's speed. Its speed may be controlled by the HGC using a six-step converter while having lower current and torque rippling. Comparisons between the BLDC with HGC and conventional converters' performance behaviours are drawn. The BLDC motor with HGBC improves the conventional converter based on a comparative investigation of the HGBC and conventional converter.

References

1. Liu, Kou-Bin, Chen-Yao Liu, Yi-Hua Liu, Yuan-Chen Chien, Bao-Sheng Wang, and Yong-Seng Wong. 2016. "Analysis and Controller Design of a Universal Bidirectional DC-DC Converter" Energies 9, no. 7: 501. https://doi.org/10.3390/en9070501

2. A. Khaligh et al., "Digital Control of an Isolated Active Hybrid Fuel Cell/Li-Ion Battery Power Supply," in IEEE Transactions on Vehicular Technology, vol. 56, no. 6, pp. 3709–3721, Nov. 2007, doi: https://doi.org/10.1109/TVT.2007.901929.
3. Huann-Keng Chiang, Bor-Ren Lin and Kuan-Wei Wu, "Study of dynamic voltage restorer under the abnormal voltage conditions," 2005 International Conference on Power Electronics and Drives Systems, Kuala Lumpur, Malaysia, 2005, pp. 308–312, doi: https://doi.org/10.1109/PEDS.2005.1619704.
4. M. S. Trivedi and R. K. Keshri, "Evaluation of Predictive Current Control Techniques for PM BLDC Motor in Stationary Plane," in IEEE Access, vol. 8, pp. 46217–46228, 2020, doi: https://doi.org/10.1109/ACCESS.2020.2978695
5. D. Mohanraj, J. Gopalakrishnan, B. Chokkalingam and L. Mihet-Popa, "Critical Aspects of Electric Motor Drive Controllers and Mitigation of Torque Ripple—Review," in IEEE Access, vol. 10, pp. 73635-73674, 2022, doi: https://doi.org/10.1109/ACCESS.2022.3187515CESS.2022.3187515.
6. H. Ardi, A. Ajami, F. Kardan and S. N. Avilagh, "Analysis and Implementation of a Nonisolated Bidirectional DC–DC Converter With High Voltage Gain," in IEEE Transactions on Industrial Electronics, vol. 63, no. 8, pp. 4878–4888, Aug. 2016, doi: https://doi.org/10.1109/TIE.2016.2552139.
7. S. K. Sahare and D. Suresh, "Modified Boost Converter-Based Speed Control of BLDC Motor," 2023 IEEE International Students' Conference on Electrical, Electronics and Computer Science (SCEECS), Bhopal, India, 2023, pp. 1–5, doi: https://doi.org/10.1109/SCEECS57921.2023.10062973.
8. H. Suryoatmojo, F. G. Cladella, V. Lystianingrum, D. C. Riawan, R. Mardiyanto and D. Ariana, "Performance of BLDC Motor Speed Control Based on Hysteresis Current Control Mechanism," 2018 International Seminar on Intelligent Technology and Its Applications (ISITIA), Bali, Indonesia, 2018, pp. 147–152, doi: https://doi.org/10.1109/ISITIA.2018.8710910.
9. P. K. Maroti, S. Padmanaban, P. Wheeler, F. Blaabjerg and M. Rivera, "Modified boost with switched inductor different configurational structures for DC-DC converter for renewable application," 2017 IEEE Southern Power Electronics Conference (SPEC), Puerto Varas, Chile, 2017, pp. 1–6, doi: https://doi.org/10.1109/SPEC.2017.8333674.